Photo-induced copper-mediated (meth)acrylate polymerization towards graphene oxide and reduced graphene oxide modification

Svitlana Railian[a], Joris J. Haven[b], Lowie Maes[a], Dries De Sloovere[c,d,e], Vanessa Trouillet[f,g], Alexander Welle[g,h], Peter Adriaensens[e,i], Marlies K. Van Bael[c,d,e], An Hardy[c,d,e], Wim Deferme[e,j], Tanja Junkers[a,b,*,1]

[a] Polymer Reaction Design Group, UHasselt – Institute for Materials Research, Agoralaan, 3590 Diepenbeek, Belgium
[b] School of Chemistry, Monash University, 19 Rainforest Walk, Clayton, VIC 3800, Australia
[c] UHasselt – Institute for Materials Research, Inorganic and Physical Chemistry, Agoralaan, 3590 Diepenbeek, Belgium
[d] Energyville, Thor Park 8320, B-3600 Genk, Belgium
[e] IMEC vzw – Division IMOMEC, Wetenschapspark 1, 3590 Diepenbeek, Belgium
[f] Institute for Applied Materials (IAM), Karlsruhe Institute of Technology (KIT), Hermann-von-Helmholtz-Platz 1, 76344 Eggenstein-Leopoldshafen, Germany
[g] Karlsruhe Nano Micro Facility (KNMF), Karlsruhe Institute of Technology (KIT), Hermann-von-Helmholtz-Platz 1, 76344 Eggenstein-Leopoldshafen, Germany
[h] Institute of Functional Interfaces, Karlsruhe Institute of Technology (KIT), Hermann-von-Helmholtz-Platz 1, 76344 Eggenstein-Leopoldshafen, Germany
[i] UHasselt – Institute for Materials Research, Nuclear Magnetic Resonance Spectroscopy Group, Agoralaan, 3590 Diepenbeek, Belgium
[j] UHasselt – Institute for Materials Research, Wetenschapspark 1, 3590 Diepenbeek, Belgium

ABSTRACT

The preparation of well-dispersed graphene/polymer nanocomposites is challenging due to the poor miscibility of graphene sheets in a polymer matrix. To enhance the interaction between both phases, graphene sheets can be decorated with polymer chains. Herein, different strategies to graft poly(methyl methacrylate) (PMMA) and poly(di(ethylene glycol) ethyl ether acrylate) (PDEGA) chains at various positions on graphene oxide and reduced graphene oxide (GO/rGO) sheets are compared. Chain attachment was achieved by "grafting-to" and "grafting-from" methods. *Grafting-to* was performed by classical copper (I)-catalyzed alkyne azide cycloaddition. Using a *grafting-from* approach, PMMA and PDEGA brushes were grown from GO and rGO sheets *via* surface-initiated photo-induced copper-mediated polymerization (SI-photoCMP). SI-photoCMP is a robust and efficient method that allows polymerizations to be carried out under mild conditions and with reduced catalyst concentration. Moreover, the successful implementation of SI-photoCMP in a continuous-flow set-up enables easy upscaling of the system and is, therefore, a more efficient and environmentally friendly process for GO/rGO surface modification. By using the *grafting-to* approach, the grafting density of PMMA (M_n = 2,600 g/mol) was one chain per 990 carbons of graphene. In contrast, longer PMMA chains (M_n = 40,300 g/mol) and higher grafting density were obtained *via* the *grafting-from* method (one PMMA chain per 140 carbons of graphene).

1. Introduction

The synthesis of novel materials with tailor made properties is essential in a variety of applications. Polymers are widely used materials. Their variety, processability, inherent mechanical properties, and light weight are highly attractive for designing new types of materials. In order to achieve tailored properties, polymers can be either molecularly modified, or be blended with another material that introduce properties that the polymer itself is lacking. Blended nanoparticles (nanofiller) in a polymer matrix, also referred to as nanocomposites, are hereby a very interesting approach [1]. One potential nanofiller that introduces sophisticated properties is graphene. Graphene has rapidly gained the attention of the scientific and industrial world after its relatively recent discovery in 2004 [2]. Its unique combination of excellent electrical, thermal, optical, and mechanical properties makes it a highly suitable material to tailor polymer nanocomposites properties [3]. The performance of polymer/graphene nanocomposites depends significantly on the dispersion of the graphene sheets in the polymer matrix. Due to Van der Waals and π π interactions, graphene sheets tend to agglomerate and phase separate on a micro and nanoscale level leading to a reduced performance of the composite. Therefore, the pre modification of graphene sheets with polymer chains is investigated to enhance the polymer/graphene miscibility.

The use of graphene through bottom up approaches is not preferred for polymer nanocomposite applications due to the high processing costs and small production scale [3]. Therefore, the focus switched to

* Corresponding author at: Polymer Reaction Design Group, UHasselt – Institute for Materials Research, Agoralaan, 3590 Diepenbeek, Belgium.
E-mail address: tanja.junkers@monash.edu (T. Junkers).

graphene oxide (GO) and reduced graphene oxide (rGO). This is mainly because of their better availability and more simple chemical functio nalization. GO has a large quantity of oxygen containing groups, such as hydroxyl and epoxy moieties, mainly situated on the basal plane of the GO sheets and carboxyl group located at the sheet edges [4]. The presence of such groups breaks, however, the aromatic structure of the sheets making GO electrically insulating. The reduction of GO by che mical, thermal or ultraviolet assisted methods allows to produce elec trically conducting rGO [5].

The covalent modification of GO/rGO surfaces with small organic molecules is based on two approaches: (i) via oxygen containing groups [6] and (ii) via sp^2 carbons from the graphene sheet [7]. Surface modification with polymers has been widely investigated [4,8]. In this regard, two main synthesis approaches are generally used, "grafting to" and "grafting from". The first is based on coupling pre synthesized polymer chains to the GO surface via efficient conjugation chemistry, whereas the latter directly grows polymers from the surface after functionalization with a suitable initiator [4,8a,8b]. In the *grafting to* approach, multiple synthesis routes are used for polymer conjugation on the surface, such as esterification [9], amidation [10], azide alkyne cycloaddition [11], nitrene cycloaddition [12], condensation reactions [13] and radical coupling [4,14]. The main advantage of this approach is the possibility to tailor and characterize the polymers before grafting them onto the surface. However, due to steric factors, lower grafting densities are achieved and longer reaction times are required due to the slow self diffusion of the polymers. In *grafting from*, polymers can be analyzed after cleavage from the surface [15] via basic hydrolysis [16], acid catalyzed transesterification [17], photo detachment [18] or an atomic force microscopy pull off method [19]. With *grafting from*, the steric effect is minimized due to the fixed position of the initiator mo lecule on the surface and fast monomer self diffusion, resulting in higher grafting densities. Polymers can be grown from the surface via conventional radical or reversible deactivation radical polymerization (RDRP) techniques. In conventional radical polymerizations, bare GO sheets have been successfully used as a radical source via opening of epoxy rings on the surface leading to the reduction of GO into rGO decorated with polymers [20]. In RDRP, polymers with predetermined molecular weight and low dispersity can be targeted [21]. Four RDRP techniques are predominantly used for GO/rGO modification: (i) single electron transfer living radical polymerization (SET LRP), (ii) atom transfer radical polymerization (ATRP), (iii) reversible addition frag mentation chain transfer polymerization (RAFT) and (iv) nitroxide mediated polymerization (NMP) [4,8]. One of the first reports on controlled surface initiated (SI) ATRP from rGO was investigated by the Nutt group where rGO was modified with 2 (4 aminophenyl)ethanol followed by the introduction of an initiator to the rGO surface [17,22]. By varying the concentration of styrene (St) monomer and the attached acrylic ATRP initiator on the surface, control over grafting densities and polymer chain length could be achieved. However, SI ATRP could only be performed at higher temperatures (110 °C in the above mentioned case of St) to initiate the polymerization reaction. Furthermore, long reaction times (10 24 h) and high CuBr/PMDETA (*N,N,N',N",N"* pen tamethyl di ethylenetriamine) concentrations were applied. Lower temperatures (65 °C) can be used to graft MMA chains using SI ATRP [23]. Lee *et al.* used SET LRP to grow St, MMA and butyl acrylate polymers from GO at 80 °C [24].

Photo induced RDRP routes have been progressively investigated for the synthesis of polymers under mild reaction conditions, mainly due to the development of highly efficient light sources (such as lasers, fluorescent lights, light emitting diodes) and the obvious environmental benefits [25]. Furthermore, photo induced reactions are highly inter esting due to the simple procedure, temporal control, and compara tively simple scalability. However, until now only little research has been performed on photo induced surface initiated polymerization on nanoparticles. UV induced SI polymerization has been reported on TiO_2 nanoparticles [26]. Also, UV induced SI ATRP was used to grow

polymer brushes from silica nanoparticles [27] and TiO_2 initiator na nowires [28]. In another approach, visible light induced SI ATRP was used to grow polymer brushes from TiO_2/rGO nanocomposites [29].

The implementation of flow chemistry for photo induced SI poly merization has many advantages such as improved safety, high re producibility, fast heat exchange, easy scalability, operation above ambient pressure boiling points of reactants and   most importantly improved homogeneous irradiation by light sources as was previously demonstrated [30]. Continuous flow synthesis is widely implemented in organic chemistry [31], and is also in polymer chemistry becoming more and more a routine technique for improving control over poly merizations. Generally, better control over polymer length and dis persity is achieved by using flow reactors [32]. The first combination of photo induced copper mediated polymerization (photoCMP) [33] and continuous flow reactors was described by Junkers and coworkers [30c,34]. photoCMP is typically applied under UV irradiation, but also visible light can be employed with the correct choice of catalyst and ligand [35]. Moreover, a number of carbon based materials was used for surface functionalization in continuous flow reactors such as full erenes [36], carbon nanotubes [37] and rGO [38]. Combination of the two approaches appears to be highly rewarding, also form the aspect of scalability of GO modifications.

In this manuscript we investigate different strategies to graft polymer brushes at different positions to graphene oxide and reduced graphene oxide (GO/rGO) sheets, on either the basal plane, sheet edges or both. To influence the dispersibility of graphene based sheets in a variety of solvents and polymer matrices, two acrylic monomers were selected for grafting: (i) the hydrophobic monomer methyl methacry late (MMA), and (ii) the more hydrophilic di(ethylene glycol) ethyl ether acrylate (DEGA). For the first time, the implementation of photoCMP as a *grafting from* procedure to grow polymer brushes from three graphene based surfaces (GO, *in situ* formed rGO and commer cially available rGO) was investigated. Polymerization reactions were performed under UV light in the presence of a copper catalyst. Copper can be disadvantageous in some biomedical applications and hence, the minimum copper concentration necessary for efficient polymer grafting was also explored. Next, a comparative study of traditional batch and flow set up on surface grafting *via* photoCMP was performed. Flow reactors allow for scalability of polymerization reactions, a well known challenge to overcome in UV induced batch polymerizations. Coupling of PMMA and PDEGA to the GO surface was explored *via* the *grafting to* approach using classical copper (I) catalyzed alkyne azide cycloaddi tion (CuAAC). Furthermore, grafting densities were compared for both approaches.

2. Results and discussion

2.1. Modification of GO/rGO surfaces

Graphene based sheets were grafted with PMMA (hydrophobic) and PDEGA (hydrophilic) to enhance the miscibility in a compatible polymer matrix. The grafted polymer chains prevent aggregation of the sheets by improving the interfacial interaction with the polymer matrix. In this manner, good dispersion can be achieved and the obtained grafted materials can be directly used as a filler in polymer nano composites. Four grafting strategies were applied to graft polymers brushes on GO and rGO surfaces, including one *grafting to* (*via* CuAAC) and three *grafting from* (*via* SI photoCMP) approaches as illustrated in Scheme 1. Grafting densities, grafting positions on the graphene sheets (basal plane, sheet edges, or both) and polymer molecular weight (distributions) were studied. In the CuAAC and SI photoCMP/1 methods (Scheme 1), the polymer chains were grafted on the sheet edges (CuAAC) and the basal plane (SI photoCMP/1) of GO by the use of the large quantity of oxygen containing groups present on the sur face. However, subsequent chemical or thermal treatment is required to recover the aromatic structure of the GO sheets in order to restore its
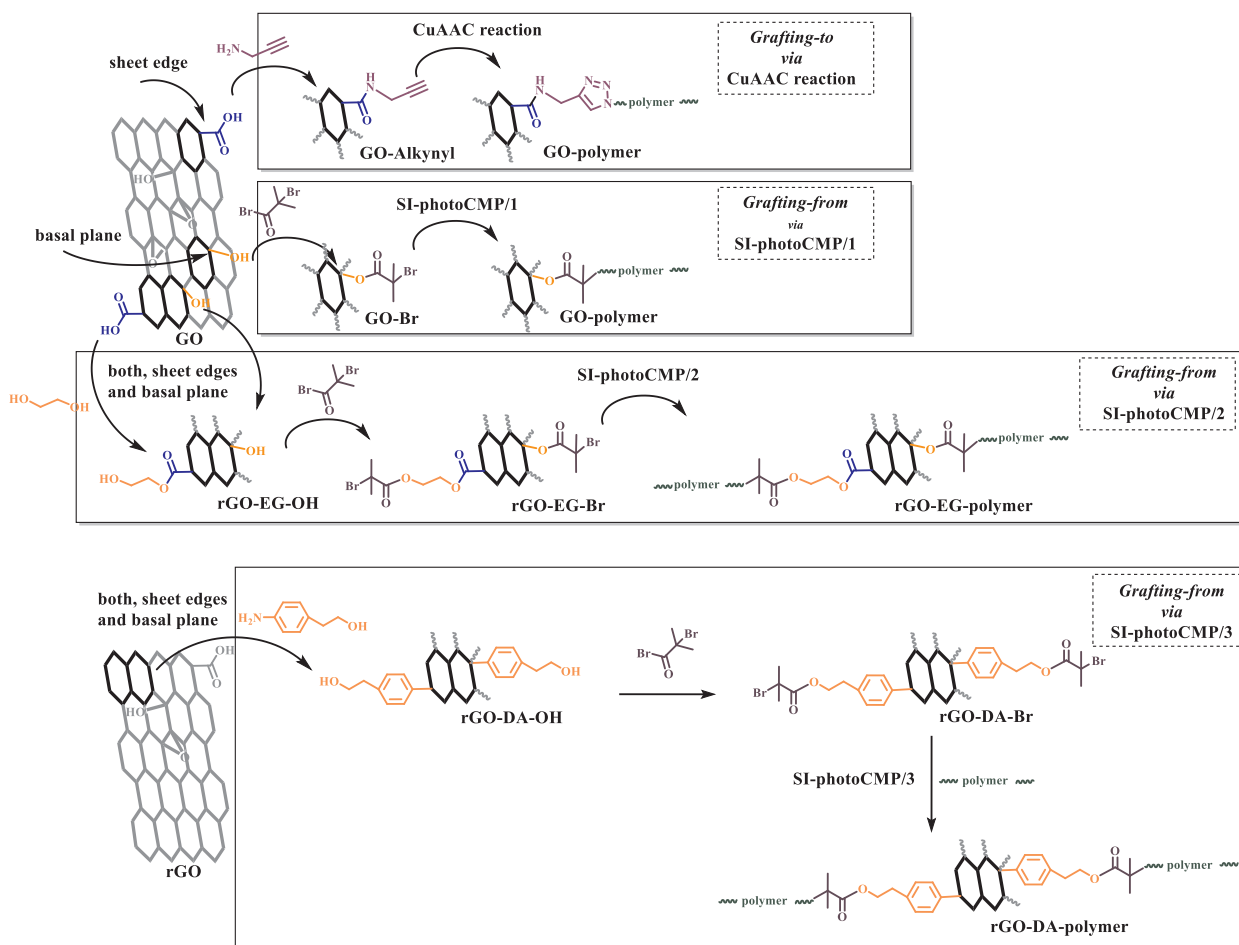
Scheme 1. General synthesis scheme of GO/rGO surface modifications.
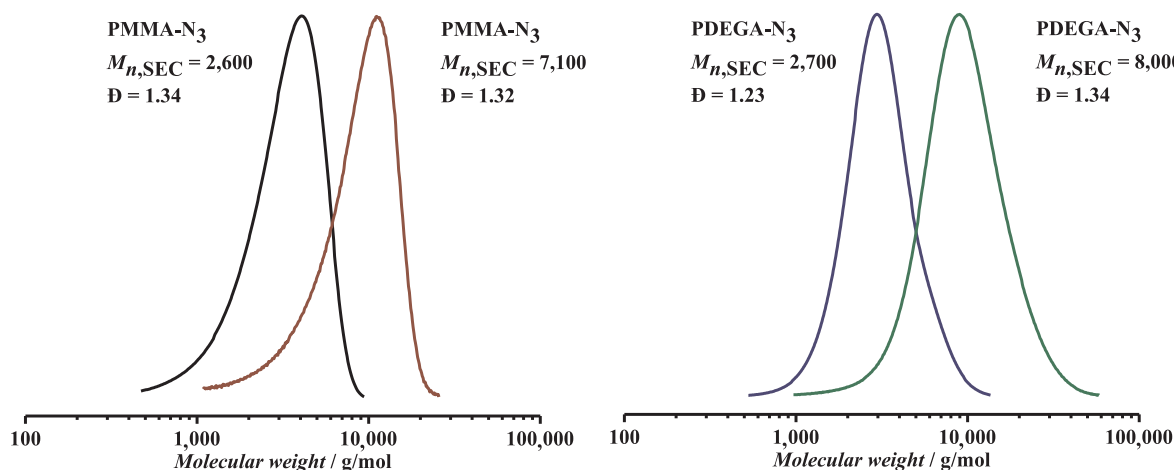

Fig. 1. SEC traces of PMMA and PDEGA used for *grafting-to* modification of GO-Alkynyl surface.

thermal and electrical properties [3]. In SI photoCMP/2 (Scheme 1), post treatment was avoided *via in situ* thermal reduction and formation of rGO prior to the polymerization step. Reduction of GO to rGO was achieved at elevated temperature of modification of carboxyl functional groups with ethylene glycol. *Via* this route, polymers can be grafted from both sheet edges and the basal plane. Thus, a high concentration of functional groups on the surface and efficient coupling of ethylene glycol is required to obtain high grafting densities. To overcome this potential limitation of SI photoCMP/2, another approach was introduced. In SI photoCMP/3, the modification of commercially

available rGO was performed by using the double bond functionalities of the sheets *via* a diazotization reaction. SI photoCMP/3 allows grafting the polymers at the sheet edges and the basal plane.

3. "Grafting-to" approach for PMMA and PDEGA attachment to GO.

Grafting to comprises a two step procedure where first alkynyl groups are attached to the GO surface, followed by CuAAC to graft the polymer chains (Scheme S1). Modification strategies have been

investigated to graft a variety of azide terminated polymer chains, such as poly(styrene) (PSt) [11], poly(N isopropyl acrylamide) (PNIPAM) [39] and poly(ethylene glycol) (PEG) [40].

Herein, to compare the influences of molecular weight on grafting, PMMA and PDEGA with different molecular weight were synthesized *via* photoCMP [41]. Four polymers were obtained and modified with azide (N_3) endgroup functionality. PMMA N_3 (M_n = 2,600 g/mol and M_n = 7,100 g/mol) and PDEGA N_3 (M_n = 2,700 g/mol and M_n = 8,000 g/mol) were obtained with dispersities (Đ) < 1.34 as analyzed *via* size exclusion chromatography (SEC, Fig. 1). The GO surface was modified *via* an amidation reaction between the carboxyl groups of GO and amino groups of propargyl amine yielding alkyne functionalities on the surface (GO Alkynyl, Scheme S1) [39]. The GO Alkynyl surface was analyzed *via* Fourier transform infrared spectroscopy (FT IR), X ray photoelectron spectroscopy (XPS) and solid state ^{13}C nuclear magnetic resonance (solid state ^{13}C NMR) to verify the successful modification (see supporting information for details). Subsequently, the CuAAC reaction was performed to graft various polymers to the GO Alkynyl sheet surface with CuBr/PMDETA as the catalyst system in dimethylformamide (DMF) (Table S3) [11,39]. As described before, the CuAAC approach only allows grafting to the sheet edges of GO where carboxyl groups are present (Scheme S1).

Thermogravimetric analysis (TGA) is a widely used technique to assess the success of polymer grafting (*i.e.* the amount of grafted polymer in wt%) or grafting density on a surface by determining the mass loss during heating on a surface by determining the mass loss during heating [42]. Grafting density is the number of bound polymers per unit surface area (*e.g.* per nm^2 or per # carbons of graphene) [43]. Fig. 2 shows the thermogravimetric profiles for the GO grafted with PMMA and PDEGA as previously described. The degree of polymer grafting was determined from the difference in weight loss between GO Alkynyl and GO PMMA or GO PDEGA at 600 °C. Such temperature (600 °C) was chosen as a point where polymers underwent thermal degradation and before substantial degradation of graphene plane. A

Fig. 2. TGA thermograms of surface-functionalized GO-PMMA and GO-PDEGA *via* CuAAC conjugation (*grafting-to* approach).

higher polymer grafting was observed for the hydrophilic PDEGA (M_n = 2,700 g/mol, 18.7 wt% grafted to GO Alkynyl), compared to PMMA (M_n = 2,600 g/mol, 9.4 wt% grafted to GO Alkynyl) which could be explained by the better solubility of PDEGA in DMF [44]. In a poor solvent the surface grafted polymer is more likely to have a mushroom structure [45] that lowers the grafting density due to steric hindrince. Based on the TGA results, higher grafting was achieved for shorter polymer chains possibly due to the lower diffusivity and increased steric hindrince for longer polymer chains [46]. The grafting efficiencies described here are in line with previously reported grafting of PSt (20% with M_n = 4,600 g/mol) [11] and PNIPAM (50% with M_n = 3,800 g/mol) using CuAAC coupling [39].

4. "Grafting-from" approach for PMMA and PDEGA growth from GO, *in situ* formed rGO and commercial rGO.

In **SI-photoCMP/1**, the GO surface was modified with a suitable ATRP initiator (see Scheme S2). An esterification reaction was performed between the hydroxyl groups of GO and acyl bromide groups of 2 bromoisobutyryl bromide resulting in GO Br [47]. XPS measurements confirmed the successful surface modification *via* the detection of Br $3d_{5/2}$ at 70.1 eV, proving the presence of covalently bound bromine with an atomic content of 0.3% (Table S1). Next, SI photoCMP was carried out under UV light (~365 nm). Polymers only grew from the basal plane of GO sheets due to the location of hydroxyl groups on the basal plane (Scheme S2).

In **SI-photoCMP/2**, the *in situ* fomation of rGO and subsequent polymer growth was investigated (Scheme S3). The presence of hydroxyl functionalities on GO surface is crucial for introducing an initiator. Additional hydroxyl groups were attached to the GO surface *via* the transformation of the existing carboxyl groups on the sheet edges into acid chlorides (*via* reaction with thionyl chloride) followed by direct quenching with ethylene glycol, followed by the *in situ* thermal reduction of the sheets (at 120 °C) and formation of rGO EG OH [23]. After introducing an initiator on the surface, the resulting rGO EG Br was used to grow polymers similar to SI photoCMP/1. *Via* this route the polymer can be grafted from both the sheet edges and basal plane of rGO (Scheme S3).

All modification steps are equally of high importance to insure successful polymer grafting. FT IR analysis of rGO EG OH shows the C H (from CH_2 O group) stretching mode vibration of the attached ethylene glycol at 2,926 cm^{-1} (Fig. S1). After modification with a suitable initiator covalently bonded Br was detected in the rGO EG Br sample (2.2 atomic %), *via* XPS, compared to 0.3 atomic % in GO Br as described in SI photoCMP/1 (Table S1). Clearly, this modification strategy is yielding better results, explained by the higher reactivity of the primary OH groups of ethylene glycols and lower reactivity of tertiary OH, directly bonded to GO surface.

SI-photoCMP/3 (Scheme S4). To also test for the grafting of commercially available rGO, a further strategy was explored. RGO has fewer hydroxyl functionalities compared to GO, and thus an additional reaction step needed to be performed to increase the abundance of OH functionalities on the surface. This was achieved by the coupling of a hydroxyl terminated molecule to the double bond functionalities of rGO. To do so, 2 (4 aminophenyl)ethanol was attached *via* a diazotization between the C(sp^2) of rGO and *in situ* generated diazonium species. The isoamyl nitrite was added to generate the diazonium salt to avoid storage of unstable and light sensitive aryl diazonium salts [22,48]. The resulting rGO DA OH sheets were further modified as above with ATRP type initiator, forming rGO DA Br. Finally, also for this substrate SI photoCMP was carried out resulting in polymers growth from both the sheet edges and basal plane of rGO (Scheme S4).

FT IR analysis shows that rGO DA OH features the desired C H (from CH_2 O group) stretching mode vibration of the attached 2 phenylethanol at 2,915 cm^{-1} (see Fig. S1). A similar Br content was detected in rGO DA Br sample (2.2 atomic %), determined by XPS,

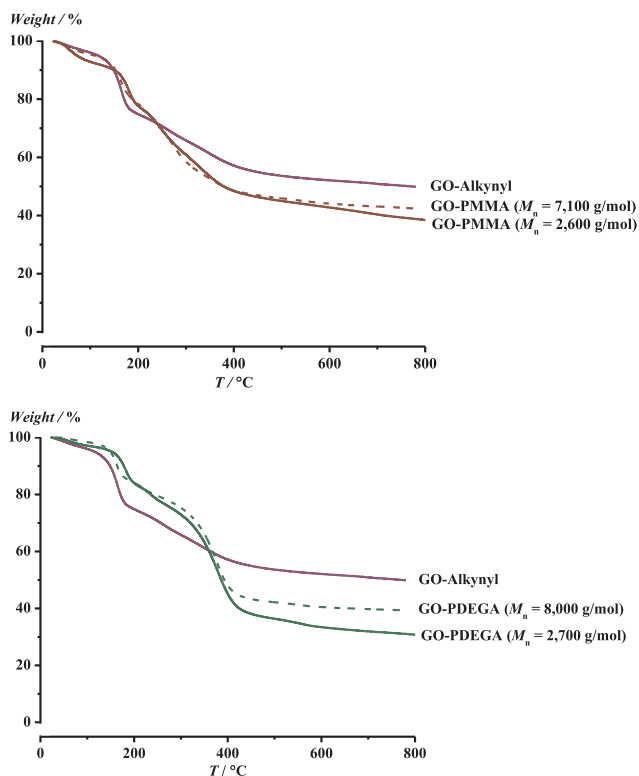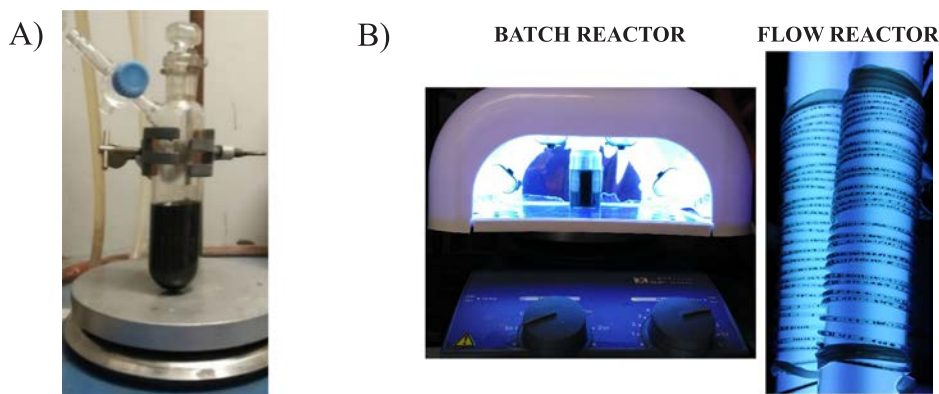**Fig. 3.** (A) Batch reactor used for alkyne-azide cycloaddition. (B) Batch and flow reactor set-ups used for SI-photoCMP.
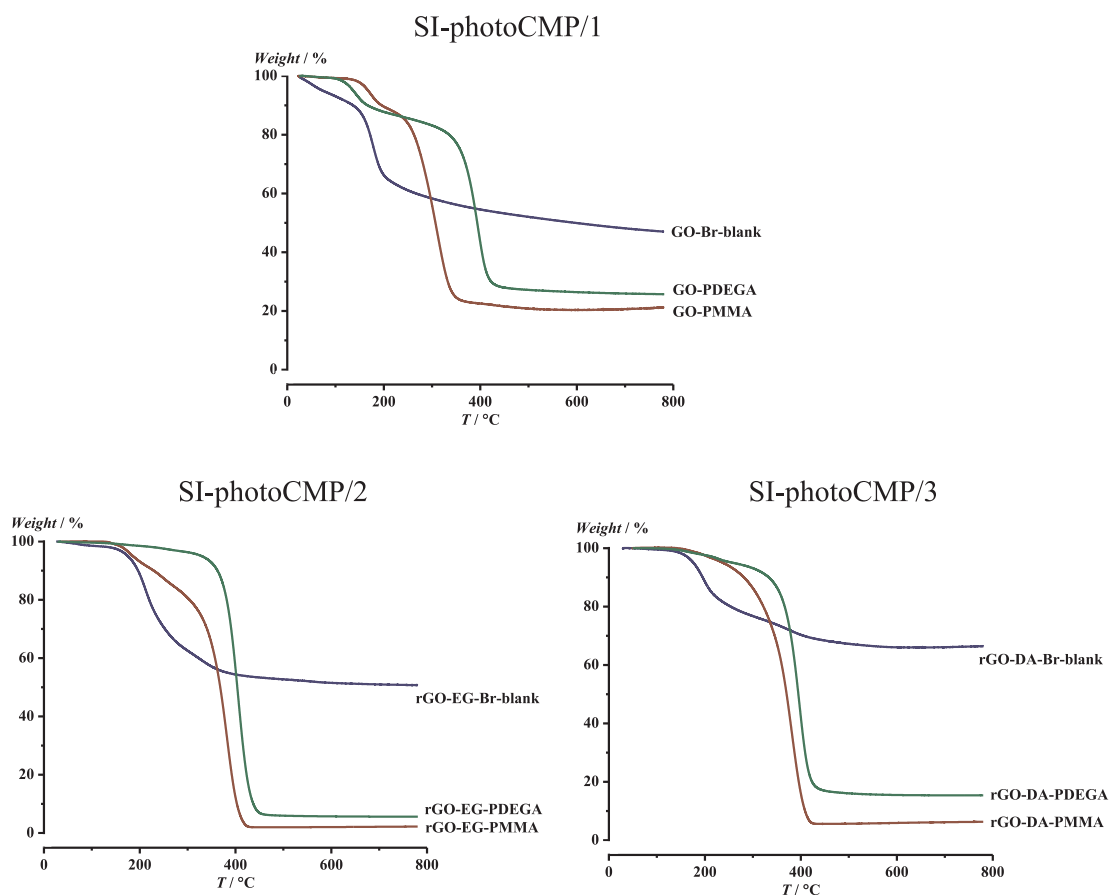

Fig. 4. TGA thermograms of PMMA and PDEGA functionalized GO/rGO sheets *via* SI-photoCMP procedures. SI-PhotoCMP was carried out in UV-batch reactor at catalyst concentrations (5.4 mmol and 7.5 mmol). The polymer-grafted samples are compared to relevant blank samples.

compared to rGO EG Br. Attachment of phenethyl alcohol was also confirmed by solid state ^{13}C NMR (appearance of the CH$_2$ resonance at 32 ppm). Modification of the surface with the bromine suitable initiator was also indicated by NMR (peak at 172 ppm assigned to the R C(O) OR functionality, see Fig. S2).

SI-photoCMP grafting reactions. As mentioned in the introduc tion, conventional ATRP was successfully applied to grow polymers from GO and rGO at elevated temperatures. By using SI photoCMP, photons from a light source can generate radicals from photoinitiators at ambient temperature [25b]. First, SI photoCMP was carried out under UV light (~365 nm) in a conventional batch reactor for 24 h. The batch reactor used for this purpose was a commercial UV nail gel curing lamp equipped with four 9 W bulbs (Fig. 3). In a batch reactor light does not penetrate deep into the reaction mixture [30c]. In addition,

GO is a relatively strong UV absorber. UV spectra of GO has a maximum absorption peak at 230 nm, attributed to π → π* transitions of aromatic C = C bonds, thus in all UV induced reactions, a fraction of the light is absorbed by GO [49]. As a consequence, longer reaction times and vigorous stirring were required to perform SI photoCMP in batch re actors. Conventional photo batch reactors do not allow for reaction upscaling since the irradiation process is hindered by the light intensity gradient in the solution.

Thus, we also investigated photografting in continuous flow reactors [30c]. To this end, the same reaction conditions were used which then resulted in only 1 h residence time (as faster reactions can be expected in continuous flow). The flow set up was custom build from gastight perfluoroalkoxy (PFA) tubing with 0.75 mm inner diameter wrapped around two UV light bulbs (alternately in a figure of eight) and a
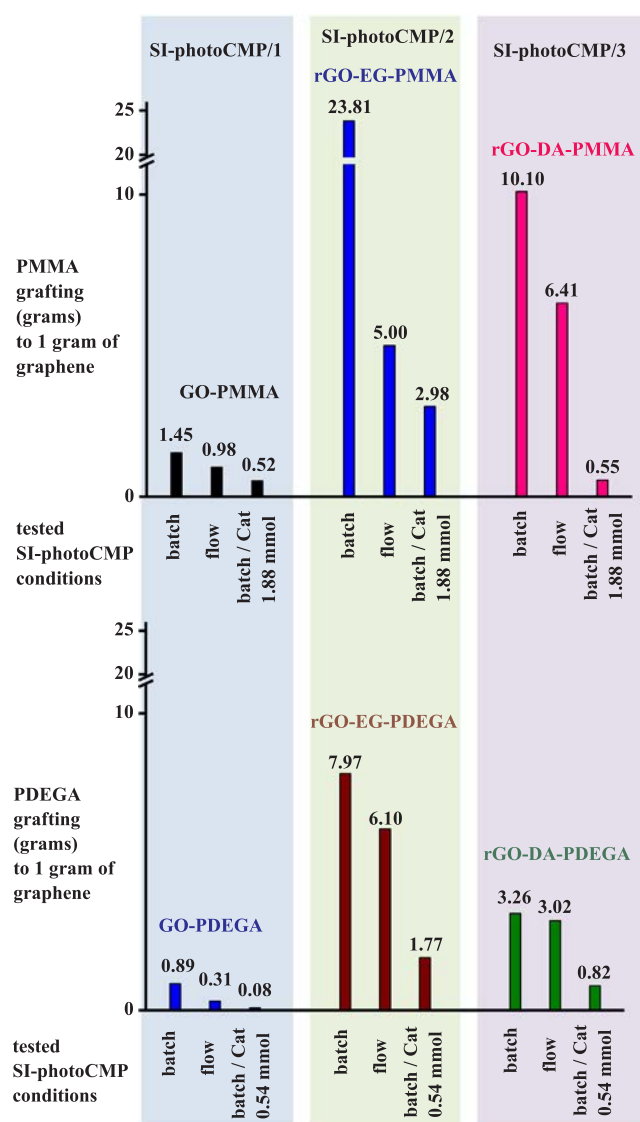
Fig. 5. Comparison of PMMA and PDEGA grafting from GO/rGO sheets *via* SI-photoCMP procedures. SI-PhotoCMP was carried out in batch, flow and batch reactor at reduced catalyst concentration. Results are obtained from TGA.

performed that followed the exact same synthesis procedure as for SI photoCMP in absence of monomer to assess the influence of UV induced GO reduction. Thus, GO Br blank, rGO EG Br blank, and rGO DA Br blank were synthesized. TGA shows the improved thermal stability of control (blank) samples, due to the partial removal of oxygen content groups from the GO/rGO surface.

First, thermograms of samples prepared in batch reactors for 24 h in the presence of catalyst (7.5 mmol for MMA grafting and 5.4 mmol for DEGA grafting) were investigated (Fig. 4). The highest polymer content was obtained for samples prepared *via* the SI photoCMP/3 method (60.1 wt% PMMA and 50.6 wt% PDEGA grafted to rGO DA Br, Table S6). The lowest polymer grafting was observed for the SI photoCMP/1 approach (29.6 wt% PMMA and 23.5 wt% PDEGA grafted to GO Br), presumably due to the comparatively low initiator concentration in these samples.

Next, 4 times (1.88 mmol for MMA grafting) and 10 times (0.54 mmol for DEGA grafting) lower catalyst concentration and ligand concentration were further investigated to minimize the amount of copper present in the residual composites. Compared to the above re sults, the thermograms showed for these cases reduced polymer grafting for all GO Initiator systems (Fig. S4), indicating the importance of sufficient catalyst concentration in reaction mixture.

The use of a continuous flow reactor in photo induced poly merizations results into better irradiation and fast polymerization of the reaction mixture [41b,51]. Scale up in flow reactors is typically achieved by using longer reactors or larger tubing diameters. SI pho toCMP was carried out in the continuous flow reactor with inner tubing diameter 0.75 mm for 1 h residence time (compared to 24 h in batch). Longer residence times are typically not favoured in flow reactors in order to keep throughput in the reactor ideal. The thermograms show similar results for the flow products as for the batch reactions (Fig. S5). Thus, a very significant improvement with respect to reaction time (> 42.9 wt% polymer grafted to rGO EG Br and rGO DA Br, Table S6) is observed for SI photoCMP/2 and SI photoCMP/3 methods in flow compared to conventional SI ATRP and SI SET LRP where the typical range of 10 24 h in batch needs to be applied [8c,22,52].

Fig. 5 summarizes the obtained results for polymer grafting towards tested SI photoCMP conditions (batch; flow and reduced catalyst con centration in batch reactors) based on TGA. Results are given as amount of polymer grafting (in grams) to 1 g of graphene as this allows for a more meaningful comparison between different types of GO/rGO. This comprises the different oxidation level of GO/rGO surfaces and length of the spacer between surface and polymer chain.

In general, the lowest polymer grafting was observed using SI photoCMP/1, compared to SI photoCMP/2,3, due to the low con centration of attached initiator. Performing SI photoCMP in a batch reactor results in the best grafting, compared to the flow reactor. The grafting reaction in flow reactor is highly efficient owing to the reaction time needed. Furthermore, performing SI photoCMP in a batch reactor at lower catalyst concentration decreases the grafting efficiency. Polymerization of acrylates monomers in solution *via* photoCMP is more efficient compared to meth(acrylates) [41b,51]. A difference that typically needs to be taken into account for polymerizing methacrylates or acrylates via photoCMP is the choice of ligand. Methacrylates show better polymerization activity with PMDETA, while acrylates are polymerized more efficiently by using Me$_6$TREN [40b]. This difference, and the generally higher rate of polymerization for acrylates, should however, not be confused with a presumably lower grafting density. Grafting efficiency is given my more than mere speed of polymeriza tion, but also by the choice of monomers, chain interactions, and lastly radical quenching by termination, which is significantly lower for me thacrylates. With this consideration, it is yet an interesting observation that almost in all tested reaction conditions, higher grafting efficiencies were achieved for MMA compared to DEGA.
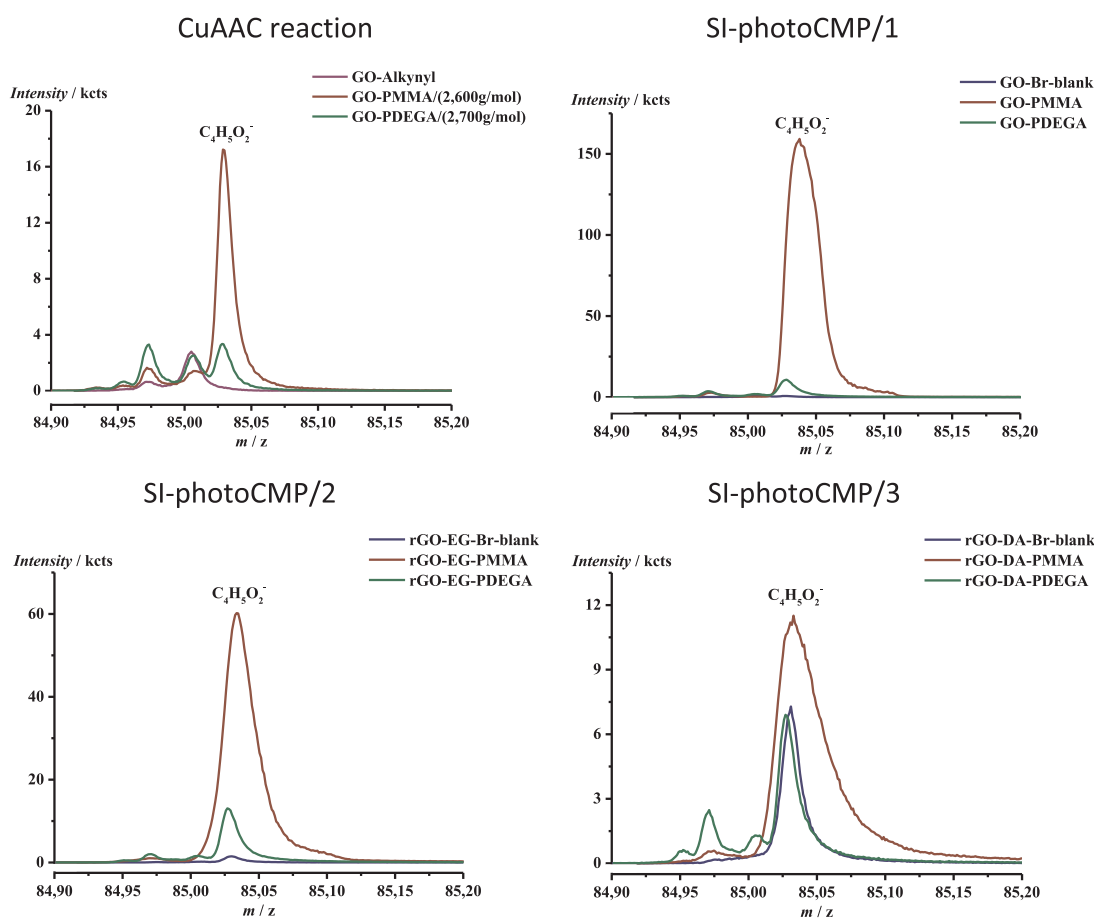
syringe pump with a 20 mL syringe (Fig. S6). Inside the syringe, six polytetrafluoroethylene coated (PTFE coated) octagonal stir bars (5 mm × 2 mm) were loaded to keep the GO Initiator well dispersed.

SI PhotoCMP of MMA from the GO initiator surface was performed in the presence of a catalyst (CuBr$_2$) and ligand (PMDETA) with a mass ratio of [GO Initiator] : [CuBr$_2$] : [PMDETA] = 1 : 0.34 : 0.85 in DMF/ MeOH. To grow DEGA from the GO Initiator surface, tris (2 (dimethy lamino)ethyl)amine (Me$_6$TREN) was used as a ligand with a mass ratio of [GO Initiator] : [CuBr$_2$] : [Me$_6$TREN] = 1 : 0.24 : 1.5. The grafting of DEGA was possible in EtOH/H$_2$O mixtures as a greener solvent alter native. It has been reported before that SI PhotoCMP can be carried out at extremely low catalyst concentration (0.137 μmol) [50]. To graft MMA, the catalyst concentration has been reduced from 7.5 mmol to 1.88 mmol (4 times below standard protocol). For DEGA grafting, 10 times lower catalyst concentration was investigated: from 5.4 mmol to 0.54 mmol. These reactions are described in Table S4.

Different from polymerization in solution, the information towards monomer conversion and the molecular weight is more difficult to obtain for surface initiated polymerization. Instead, polymer grafting was calculated from TGA to estimate the success of SI photoCMP at different reaction conditions. Additionally, control experiments were

Fig. 6. ToF-SIMS spectra of $C_4H_5O_2^-$ fragment of PMMA and PDEGA functionalized GO/rGO sheets *via* CuAAC reaction and SI-photoCMP procedures. Spectra compared to relevant blank samples.

5. Detailed investigation of polymer grafting to GO/rGO surfaces (FT-IR, XPS, ToF-SIMS, quantitative solid-state ^{13}C NMR).

FT IR, XPS, time of flight secondary ion mass spectrometry (ToF SIMS) and solid state ^{13}C NMR analysis were performed to in detail to further investigate the polymer grafting for both *grafting to* and *grafting from* approaches. For *grafting to via* CuAAC, GO PMMA (with PMMA M_n = 2,600 g/mol) and GO PDEGA (with PMMA M_n = 2,700 g/mol) were investigated since they showed the highest grafting ratios ac cording to TGA. For *grafting from*, PMMA and PDEGA grafted *via* SI photoCMP/1 3 in a batch reactor were analyzed. All samples were compared to relevant blank GO/rGO Initiator samples.

FT IR provides qualitative information towards polymer grafting. GO sheets that were modified with PMMA and PDEGA chains show additional signals that can be directly assigned to the polymer stretching modes as shown in Fig. S7. FT IR confirms presence of the grafts on the GO sheets.

Further analysis was performed *via* ToF SIMS which is very surface sensitive technique with a probing depth of a few nm only. The mass spectra obtained by ToF SIMS allow for a differentiation of several polymer layers based on characteristic molecular fragments. In this case, amongst several other, the $C_4H_5O_2$ fragment attributed to PMMA and the C_2H_3O fragment attributed to PDEGA were detected. Fig. 6 shows the intensity of the detected $C_4H_5O_2$ fragment for the different GO/rGO derivatives. Since methyl methacrylates yield $C_4H_5O_2$ frag ments among several other characteristic signals in SIMS, the highest intensity was observed for all GO PMMA based samples, proving the presence of PMMA on the surface. Differently, the side chain of grafted PDEGA yields strong C_2H_3O signals, which is not applicable for grafted

PMMA. After comparison the intensities of C_2H_3O fragments (Fig. 7), the highest was obtained for all GO PDEGA based samples, proving the presence of PDEGA on the surface.

The high resolution C 1s XPS spectra of the grafted polymers are depicted in Fig. 8. The appearance of a C Br signal at 70.1 eV (not shown, Br atomic % is represented instead in Table S1) confirms the successful introduction of an initiator molecule on the GO/rGO surface, as discussed above. After introducing the PMMA chains on the surface, the C 1s XPS spectra of the new materials can be deconvoluted into three components, C C/C H, C O and O = C O species at 285.0, 286.6, and 288.8 eV respectively, in accordance with the chemical composi tion of the grafted polymer. The close matching between the theoretical (3 : 1 : 1) and measured/fitted values in C 1s peak confirms the at tachment of PMMA on the surface (Table S8). However, poor matching of C O peaks in GO PMMA (M_n = 2,600 g/mol) sample was observed and can be explained by a low grafting density and therefore a signal stemming from both, PMMA and GO Alkynyl. For PDEGA, the C 1s XPS spectra can be deconvoluted into three components, similar to PMMA but with given theoretical ratios 3 : 5 : 1, based on carbon chemical environment of PDEGA. Again, a close match between the theoretical and measured/fitted values was obtained for samples grafted with PDEGA (Table S8).

In a last step, solid state ^{13}C NMR spectra were measured to analyze the structures of all GO/rGO derivatives after grafting (Fig. S8). In GO PMMA, the appearance of additional resonance peaks are assigned to backbone CH_3 at 16 ppm, the quaternary C and CH_2 backbone at 45 ppm, O CH_3 at 52 ppm and R C(O) OR at 178 ppm [53]. In GO PDEGA, resonance signals of PDEGA chains are assigned to CH_3 at 15 ppm, CH and CH_2 backbone at 41 ppm, O CH_2 at 69 ppm and R
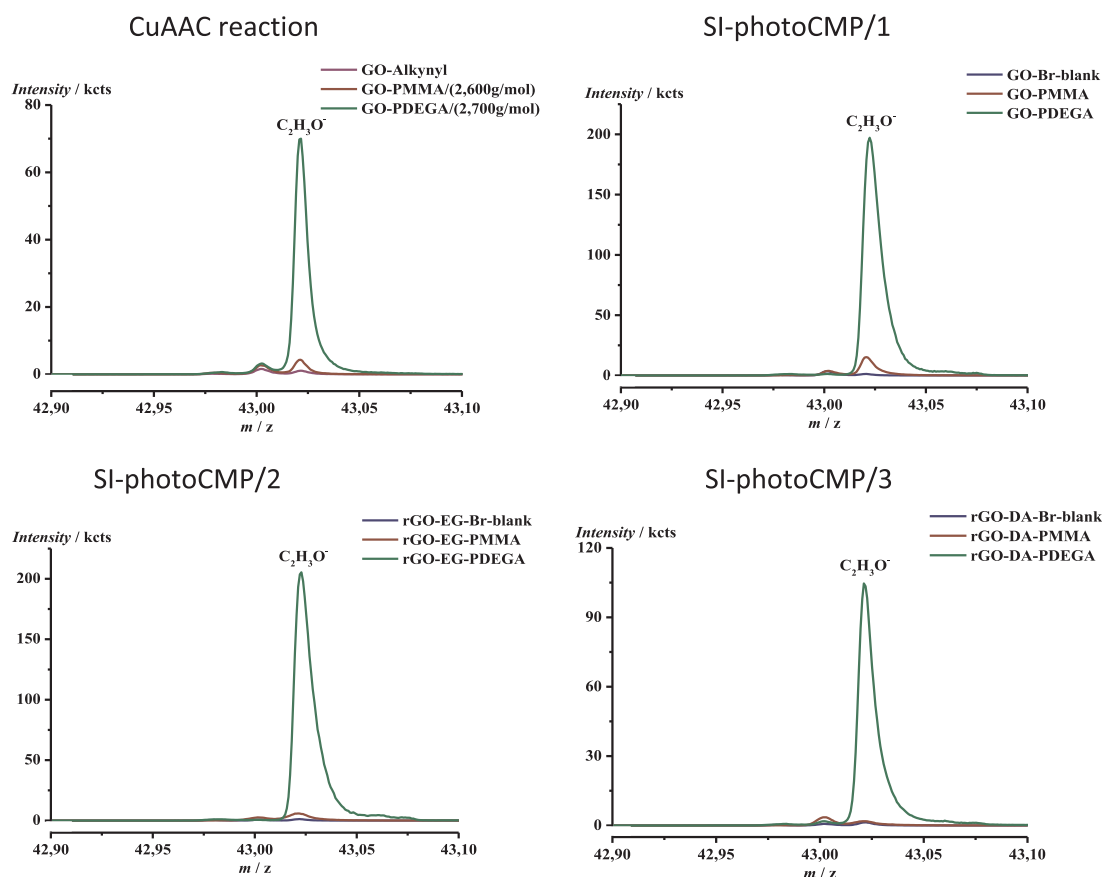
Fig. 7. ToF-SIMS spectra of C$_2$H$_3$O fragment of PMMA and PDEGA functionalized GO/rGO sheets *via* CuAAC reaction and SI-photoCMP procedures. Spectra are compared to relevant blank samples.

C(O) OR at 174 ppm. In the blank samples of ^{13}C NMR spectra, no high intensity resonance signals from impurities were detected. It proves reliable TGA thermogram interpretation over mass loss and quantitative determination of polymer grafting on the GO/rGO surfaces.

6. Determination of the polymer grafting densities of GO/rGO surfaces from TGA.

To calculate the polymer grafting density on GO/rGO surfaces, first the graft chain length needs to be determined. While it is straightforward to characterize the average length and dispersity of the polymer chains in *grafting to*, the same information is more cumbersome to obtain for *grafting from* methods. To this end, grafted polymers were cleaved from the modified GO/rGO surfaces *via* base hydrolysis (to break the ester linkage) in order to analyze the molecular weight (distributions) [16]. Due to the minimized steric effect [4,8a,8b], longer polymer chains are expected compared to *grafting to*. PMMA was cleaved from GO PMMA, rGO EG PMMA and rGO DA PMMA, synthesized *via* SI photoCMP/1 3 in a batch reactor. As a side reaction, ester groups present in the PMMA side chains (methyl group) are prone to hydrolyse under basic conditions, and therefore, were quenched *in situ* with methanol to restore the methyl ester side chains. Cleavage of PDEGA was not performed due to the longer and complexer side chains.

Fig. S9 shows SEC analysis of the cleaved PMMA obtained from GO PMMA, rGO EG PMMA and rGO DA PMMA UV batch polymerizations (7.5 mmol catalyst concentration). The average number molecular weights (M_n) observed were 35,200 g/mol, 40,300 g/mol and 29,200 g/mol respectively. Dispersities of the cleaved PMMA were observed in the range of Đ = 1.40 (GO PMMA) and Đ =1.59 (rGO EG PMMA). The PMMA cleaved from rGO EG PMMA has higher dispersity and the high molecular weight shoulder, explained by an increase of

viscosity, which causes a reduced stirring speed. Light does not penetrate deep through the mixture and polymerization occurs only at the irradiated parts. Therefore, a high stirring speed and efficient mixing is required. In addition, higher viscosity favors bimolecular radical termination events of growing polymer chains on the surface. PMMA has higher molecular weight brushes compared to PMMA, used in CuAAC. However, broader dispersities were observed by using SI photoCMP to polymerize from the surface, compared to previously reported PMMA grafting *via* conventional thermally intiated SI ATRP with M_n = 1,170 g/mol and Đ = 1.09 [23].

The grafting density is defined as a number of attached polymer chains per unit surface area. The polymer grafting density on the surface was determined by TGA. Herein, the grafting density is shown as # carbons of graphene per grafted one polymer chain. By knowing the area of the benzene ring in graphene (0.0524 nm^2), the grafting density as a number of polymer chains per nm^2 of graphene can be calculated (Table 1) [54].

As discussed previously, in *grafting to*, higher molecular weight polymers have slower diffusivity that results into lower grafting ratio [46]. Here, one PMMA chain (M_n = 2,600 g/mol) was grafted per 990 carbons of graphene and one PMMA chain (M_n = 7,100 g/mol) was grafted per 3,251 carbons of graphene (Table 1). A lower grafting efficiency was previously reported by using CuAAC conjugation where one PSt (M_n = 4,600 g/mol) chain was grafted to approximately 1,500 carbon atoms of graphene [11]. In another contribution, the CuAAC conjugation approach resulted in one PMMA chain (M_n = 2,415 g/mol) per 5,000 carbons of graphene [54].

In general, higher grafting density is achieved using *grafting from* approach, compared to *grafting to*. Thus, one PMMA chain (M_n = 2,600 g/mol) was grafted per 990 carbons of graphene in CuAAC, while one PMMA chain (M_n = 40,300 g/mol) per 140 and one
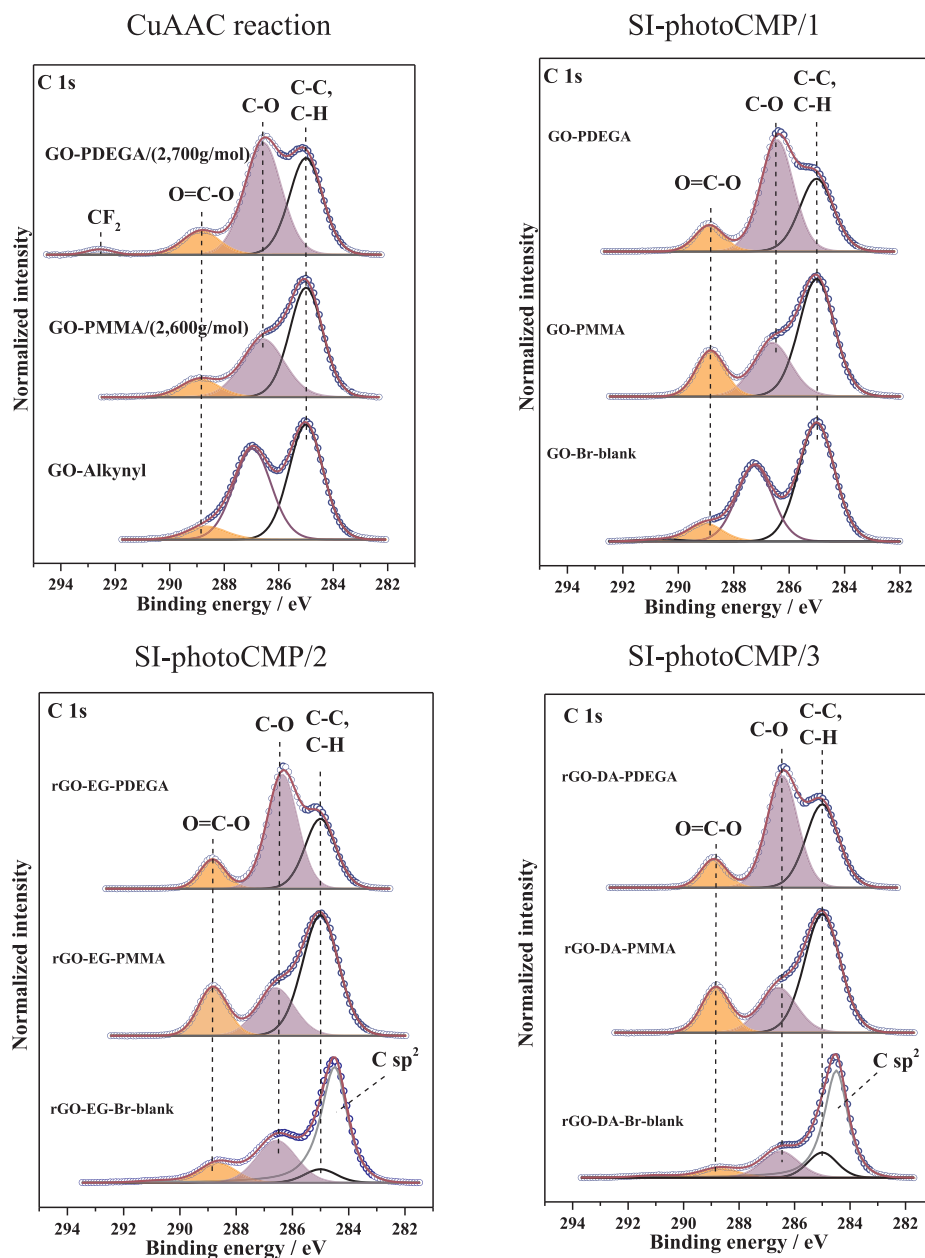
Fig. 8. XPS spectra of PMMA and PDEGA functionalized GO/rGO sheets *via* CuAAC reaction and SI-photoCMP procedures. Spectra compared to relevant blank samples. The CF2 signal in the CuAAC reaction stems from sample contamination.

Table 1
Overview of grafting characteristics from the various methods used, determined from TGA.

Sample	M_{nSEC}, (PMMA) g/mol	# carbons of graphene per grafted PMMA chain	# PMMA chains per nm² of graphene
GO-PMMA/(2,600 g/mol)	2,600	990	0.12
GO-PMMA/(7,100 g/mol)	7,100	3,251	0.04
GO-PMMA (SI-photoCMP/1)	35,200	2,010	0.06
rGO-EG-PMMA (SI-photoCMP/2)	40,300	140	0.82
rGO-DA-PMMA (SI-photoCMP/3)	29,200	248	0.46
GO-PDEGA/(2,700 g/mol)	2,700	403	0.28
GO-PDEGA/(8,000 g/mol)	8,000	2,321	0.05

PMMA (M_n = 29,200 g/mol) per 248 carbons of graphene was grafted *via* SI photoCMP/2 and SI photoCMP/3, respectively. Those obtained grafting densities are much higher than previously reported SI ATRP grafting results of one PSt chain (M_n = 60,000 g/mol) per 1,000 carbon atoms [22]. Differing from the general trend, less PMMA grafting was obtained using SI photoCMP/1. Here, one PMMA chain was grafted per 990 and 2,010 carbons of graphene *via* CuAAC and SI photoCMP/1, respectively (Table 1). This can be explained by the difference in grafted PMMA molecular weight of M_n = 2,600 g/mol (CuAAC) and M_n = 35,200 g/mol (SI photoCMP/1) and low initiator concentration attached to the GO surface. It should be noted that the outcome of the grafting experiments also depends on the GO used in the respective
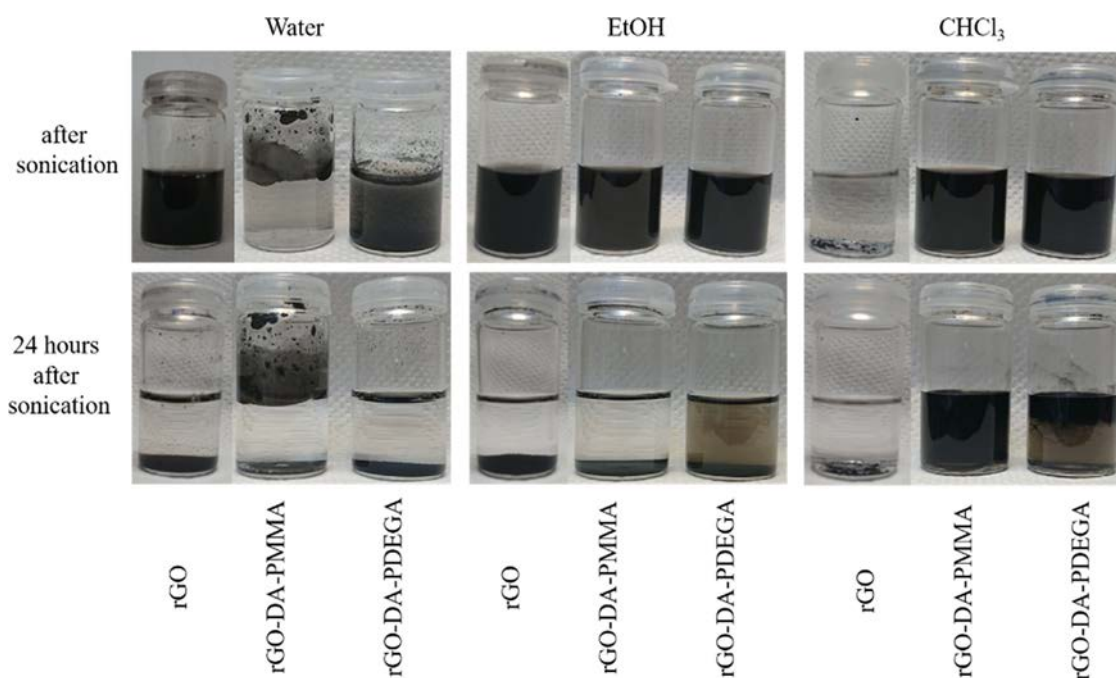
Fig. 9. Dispersions of rGO, rGO-DA-PMMA and rGO-DA-PDEGA in various solvents with a concentration of 1 mg/mL.

experiments, since GO is a relatively heterogeneous material. To make data comparable, the above values are determined on the same batches of GO. Yet, tests with different batches of GO showed that the method is overall well reproducible and significant.

6.1. Dispersibility studies

Properties such as the dispersibility of GO/rGO derivatives in a variety of solvents and matrixes can be optimized by tuning polymer type and molecular weight. The dispersibility of rGO compared to GO is poor in organic solvents. Thus, the influence on the dispersibility of rGO sheets was investigated after polymerization with hydrophobic PMMA and hydrophilic PDEGA chains *via* SI photoCMP/3. RGO, rGO DA PMMA and rGO DA PDEGA were dispersed in deionized water, ethanol (EtOH), and chloroform (CHCl$_3$) *via* sonication (15 min, Fig. 9). RGO DA PMMA is not dispersible in polar solvents (water) but has enhanced dispersibility in nonpolar solvents like chloroform (see Fig. 9). Even 24 h after sonication the PMMA modified sheets of rGO did not pre cipitate. In contrast, PDEGA is a more polar compared to PMMA. As a result, rGO DA PDEGA became better dispersible in ethanol as observed in Fig. 9.

7. Conclusions

The grafting of GO and rGO sheets with hydrophobic (PMMA) and hydrophilic (PDEGA) polymer chains *via* one *grafting to* and three *grafting from* approaches was investigated. SI PhotoCMP proved a great tool for the synthesis of rGO polymer materials under mild conditions (UV irradiation instead of elevated temperatures) with high polymer grafting density. The polymers were also grafted at reduced catalyst concentration (10 times for DEGA and 4 times for MMA grafting below standard protocol). In addition, the possibility to perform SI photoCMP in both batch and continuous flow reactors was demonstrated. Using a continuous flow reactor allows to reduce the reaction time (from 24 h to 1 h) and upscale the system. Higher grafting densities were achieved by using *grafting from* techniques (SI photoCMP/2,3) due to the mini mized steric factor compared to *grafting to via* CuAAC. One PMMA chain (M_n = 2,600 g/mol) was grafted per 990 carbons of graphene *via* the *grafting to* approach, calculated by TGA. In contrast, *via* SI photoCMP,

longer PMMA chains (M_n = 40,300 g/mol) and a higher grafting density (one PMMA chain per 140 carbons of graphene) were obtained. The PMMA grafted rGO has improved dispersibility in chloroform, compared to initial rGO, whilst grafted PDEGA to rGO has improved dispersibility in ethanol. The proposed SI photoCMP technique com prises mild reaction conditions, short reaction time (1 h in flow reactor) and high grafting densities with potential scalability. The pre grafted polymer chains on the rGO surface improve its dispersibility in solvents and potentially in suitable polymer matrixes for production of evenly dispersed graphene sheets in polymer nanocomposites.

CRediT authorship contribution statement

Svitlana Railian: Conceptualization, Methodology, Investigation, Data curation, Writing original draft, Visualization. **Joris J. Haven:** Writing review & editing, Validation. **Lowie Maes:** Formal analysis, Data curation. **Dries De Sloovere:** Investigation, Resources. **Vanessa Trouillet:** Investigation, Formal analysis, Resources. **Alexander Welle:** Investigation, Formal analysis, Resources. **Peter Adriaensens:** Investigation, Formal analysis, Resources. **Marlies K. Van Bael:** Formal analysis. **An Hardy:** Formal analysis. **Wim Deferme:** Supervision, Funding acquisition, Project administration. **Tanja Junkers:** Writing review & editing, Conceptualization, Methodology, Resources, Supervision, Project administration, Funding acquisition.

Declaration of Competing Interest

The authors declare that they have no known competing financial interests or personal relationships that could have appeared to influ ence the work reported in this paper.

based composites" for which funding was received from VLAIO with grant number 140818.

Data availability

References

[1] (a) J.H. Koo, Polymer nanocomposites, McGraw-Hill Professional Pub., 2006. (b) H. Fischer, Materials Science and Engineering: C 2003, 23, 763–772. (c) F. Hussain, M. Hojjati, M. Okamoto, R.E. Gorga, J. Compos. Mater. 2006, 40, 1511–1575.

[2] K.S. Novoselov, A.K. Geim, S.V. Morozov, D. Jiang, Y. Zhang, S.V. Dubonos, I.V. Grigorieva, A.A. Firsov, Science 306 (2004) 666–669.

[3] H. Kim, A.A. Abdala, C.W. Macosko, Macromolecules 43 (2010) 6515–6530.

[4] H.J. Salavagione, G. Martínez, G. Ellis, Macromol. Rapid Commun. 32 (2011) 1771–1789.

[5] S. Park, R.S. Ruoff, Nat. Nanotechnol. 4 (2009) 217.

[6] D.R. Dreyer, S. Park, C.W. Bielawski, R.S. Ruoff, Chem. Soc. Rev. 39 (2010) 228–240.

[7] a) L. Rodriguez-Perez, M.Á. Herranz, N. Martin, Chem. Commun. 49 (2013) 3721–3735;
b) A. Kasprzak, A. Zuchowska, M. Poplawska, Beilstein J. Org. Chem. (2018) 14.

[8] a) A. Badri, M.R. Whittaker, P.B. Zetterlund, J. Polym. Sci., Part A: Polym. Chem. 50 (2012) 2981–2992;
b) R.K. Layek, A.K. Nandi, Polymer 54 (2013) 5087–5103;
c) A.S. Nia, W.H. Binder, Prog. Polym. Sci. 67 (2017) 48–76.

[9] H.J. Salavagione, M.A. Gomez, G. Martinez, Macromolecules 42 (2009) 6331–6334.

[10] Z. Liu, J.T. Robinson, X. Sun, H. Dai, J. Am. Chem. Soc. 130 (2008) 10876–10877.

[11] S. Sun, Y. Cao, J. Feng, P. Wu, J. Mater. Chem. 20 (2010) 5605–5607.

[12] H. He, C. Gao, Chem. Mater. 22 (2010) 5054–5064.

[13] Z. Xu, C. Gao, Macromolecules 43 (2010) 6716–6723.

[14] L. Kan, Z. Xu, C. Gao, Macromolecules 44 (2010) 444–452.

[15] J.O. Zoppe, N.C. Ataman, P. Mocny, J. Wang, J. Moraes, H.-A. Klok, Chem. Rev. 117 (2017) 1105–1318.

[16] D. Baskaran, J.W. Mays, M.S. Bratcher, Angew. Chem. 116 (2004) 2190–2194.

[17] M. Fang, K. Wang, H. Lu, Y. Yang, S. Nutt, J. Mater. Chem. 20 (2010) 1982–1992.

[18] X. Xiong, L. Xue, J. Cui, ACS Macro Lett. 7 (2018) 239–243.

[19] D. Goodman, J.N. Kizhakkedathu, D.E. Brooks, Langmuir 20 (2004) 6238–6245.

[20] a) R. Feng, W. Zhou, G. Guan, C. Li, D. Zhang, Y. Xiao, L. Zheng, W. Zhu, J. Mater. Chem. 22 (2012) 3982–3989;
b) M. Kim, C. Lee, Y.D. Seo, S. Cho, J. Kim, G. Lee, Y.K. Kim, J. Jang, Chem. Mater. 27 (2015) 6238–6248.

[21] M.H. Stenzel, C. Barner-Kowollik, Mater. Horiz. 3 (2016) 471–477.

[22] M. Fang, K. Wang, H. Lu, Y. Yang, S. Nutt, J. Mater. Chem. 19 (2009) 7098–7105.

[23] G. Goncalves, P.A.A.P. Marques, A. Barros-Timmons, I. Bdkin, M.K. Singh, N. Emami, J. Gracio, J. Mater. Chem. 20 (2010) 9927–9934.

[24] S.H. Lee, D.R. Dreyer, J. An, A. Velamakanni, R.D. Piner, S. Park, Y. Zhu, S.O. Kim, C.W. Bielawski, R.S. Ruoff, Macromol. Rapid Commun. 31 (2010) 281–288.

[25] a) X. Pan, M.A. Tasdelen, J. Laun, T. Junkers, Y. Yagci, K. Matyjaszewski, Prog. Polym. Sci. 62 (2016) 73–125;
b) N. Corrigan, J. Yeow, P. Judzewitsch, J. Xu, C.A.J.M. Boyer, Angew. Chem. (2018).

[26] H. Kong, J. Song, J. Jang, Environ. Sci. Technol. 44 (2010) 5672–5676.

[27] P. Liu, J. Tian, W. Liu, Q. Xue, Polym. Int. 53 (2004) 127–130.

[28] J. Yan, B. Li, F. Zhou, W. Liu, ACS Macro Lett. 2 (2013) 592–596.

[29] A. Bansal, A. Kumar, P. Kumar, S. Bojja, A.K. Chatterjee, S.S. Ray, S.L. Jain, RSC Adv. 5 (2015) 21189–21196.

[30] (a) E. Baeten, J.J. Haven, T. Junkers, Polym. Chem. 8 (2017) 3815–3824. (b) J. Wegner, S. Ceylan, A. Kirschning, Chem. Commun. 47 (2011) 4583–4592. (c) T. Junkers, B. Wenn, Reaction Chem. & Eng. 1 (2016) 60–64.

[31] a) K. Jähnisch, V. Hessel, H. Löwe, M. Baerns, Angew. Chem. Int. Ed. 43 (2004) 406–446;
b) A. Kirschning, W. Solodenko, K. Mennecke, Chem.–A, Eur. J. 12 (2006) 5972–5990;
c) B.P. Mason, K.E. Price, J.L. Steinbacher, A.R. Bogdan, D.T. McQuade, Chem. Rev. 107 (2007) 2300–2318;
d) R.L. Hartman, K.F. Jensen, Lab Chip 9 (2009) 2495–2507;
e) C. Wiles, P. Watts, Eur. J. Org. Chem. 2008 (2008) 1655–1671;
f) K. Geyer, T. Gustafsson, P.H. Seeberger, Synlett 2009 (2009) 2382–2391;
g) D. Webb, T.F. Jamison, Chem. Sci. 1 (2010) 675–680.

[32] a) J.J. Haven, T. Junkers, Chimica Oggi/Chemistry Today 36 (2018) 42–44;
b) J.J. Haven, T. Junkers, Eur. J. Org. Chem. 2017 (2017) 6474–6482;
c) M. Rubens, J.H. Vrijsen, J. Laun, T. Junkers, Angew. Chem. Int. Ed. 58 (2019) 3183–3187;
d) X. Hu, N. Zhu, Z. Fang, Z. Li, K. Guo, Eur. Polym. J. 80 (2016) 177–185.

[33] a) A. Anastasaki, V. Nikolaou, Q. Zhang, J. Burns, S.R. Samanta, C. Waldron, A.J. Haddleton, R. McHale, D. Fox, V. Percec, P. Wilson, D.M. Haddleton, J. Am. Chem. Soc. 136 (2014) 1141–1149;
b) M. Rolland, R. Whitfield, D. Messmer, K. Parkatzidis, N.P. Truong, A. Anastasaki, ACS Macro Lett. 8 (2019) 1546–1551;
c) D. Konkolewicz, K. Schröder, J. Buback, S. Bernhard, K. Matyjaszewski, ACS Macro Lett. 1 (2012) 1219–1223;
d) R. Whitfield, K. Parkatzidis, M. Rolland, N.P. Truong, A. Anastasaki, Angew. Chem. Int. Ed. 58 (2019) 13323–13328.

[34] N. Zhu, X. Hu, Z. Fang, K. Guo, ChemPhotoChem 2 (2018) 831–838.

[35] G. Ramakers, A. Krivcov, V. Trouillet, A. Welle, H. Möbius, T. Junkers, Macromol. Rapid Commun. 38 (2017) 1700423.

[36] a) E. Rossi, T. Carofiglio, A. Venturi, A. Ndobe, M. Muccini, M. Maggini, Energy Environ. Sci. 4 (2011) 725–727;
b) H. Seyler, W.W. Wong, D.J. Jones, A.B. Holmes, J. Org. Chem. 76 (2011) 3551–3556;
c) S. Silvestrini, D. Dalle Nogare, T. Carofiglio, E. Menna, P. Canu, M. Maggini, Eur. J. Org. Chem. (2011, 2011) 5571–5576.

[37] a) P. Salice, D. Fenaroli, C.C. De Filippo, E. Menna, G. Gasparini, M. Maggini, chimica oggi/Chemistry, Today (2012) 30;
b) P. Salice, E. Rossi, A. Pace, P. Maity, T. Carofiglio, E. Menna, M. Maggini, J. Flow Chem. 4 (2014) 79–85;
c) J.H. Bartha-Vári, M.I. Toşa, F.D. Irimie, D. Weiser, Z. Boros, B.G. Vértessy, C. Paizs, L. Poppe, ChemCatChem 7 (2015) 1122–1128;
d) S. Melendi, S. Bonyadi, P. Castell, M. Martinez, M. Mackley, Chem. Eng. Sci. 84 (2012) 544–551;
e) P. Salice, P. Maity, E. Rossi, T. Carofiglio, E. Menna, M. Maggini, Chem. Commun. 47 (2011) 9092–9094.

[38] S. Silvestrini, C.C. De Filippo, N. Vicentini, E. Menna, R. Mazzaro, V. Morandi, L. Ravotto, P. Ceroni, M. Maggini, Chem. Mater. 30 (2018) 2905–2914.

[39] Y. Pan, H. Bao, N.G. Sahoo, T. Wu, L. Li, Adv. Funct. Mater. 21 (2011) 2754–2763.

[40] Z. Jin, T.P. McNicholas, C.-J. Shih, Q.H. Wang, G.L. Paulus, A.J. Hilmer, S. Shimizu, M.S. Strano, Chem. Mater. 23 (2011) 3362–3370.

[41] (a) Y.-M. Chuang, B. Wenn, S. Gielen, A. Ethirajan, T. Junkers, Polym. Chem. 6 (2015) 6488–6497;
(b) S. Railian, B. Wenn, T. Junkers, J. Flow Chem. 6 (2016) 260–267.

[42] (a) A. Coats, J. Redfern, Analyst 88 (1963) 906–924;
(b) K. Chrissafis, D. Bikiaris, Thermochim. Acta 523 (2011) 1–24.

[43] D.N. Benoit, H. Zhu, M.H. Lilierose, R.A. Verm, N. Ali, A.N. Morrison, J.D. Fortner, C. Avendano, V.L. Colvin, Anal. Chem. 84 (2012) 9238–9245.

[44] T. Wu, K. Efimenko, J. Genzer, J. Am. Chem. Soc. 124 (2002) 9394–9395.

[45] L.C. Moh, M.D. Losego, P.V. Braun, Langmuir 27 (2011) 3698–3702.

[46] M. Kim, S. Schmitt, J. Choi, J. Krutty, P. Gopalan, Polymers 7 (2015) 1346–1378.

[47] M. Peeters, S. Kobben, K. Jiménez-Monroy, L. Modesto, M. Kraus, T. Vandenryt, A. Gaulke, B. van Grinsven, S. Ingebrandt, T. Junkers, Sens. Actuators, B 203 (2014) 527–535.

[48] J.L. Bahr, J.M. Tour, Chem. Mater. 13 (2001) 3823–3824.

[49] E. Rommozzi, M. Zannotti, R. Giovannetti, C. D'Amato, S. Ferraro, M. Minicucci, R. Gunnella, A. Di Cicco, Catalysts 8 (2018) 598.

[50] J. Laun, M. Vorobii, A. de los Santos Pereira, O. Pop-Georgievski, V. Trouillet, A. Welle, C. Barner-Kowollik, C. Rodriguez-Emmenegger, T. Junkers, Macromolecul. Rapid Commun. 36 (2015) 1681–1686.

[51] B. Wenn, M. Conradi, A.D. Carreiras, D.M. Haddleton, T. Junkers, Polym. Chem. 5 (2014) 3053–3060.

[52] (a) K. Qi, Y. Sun, H. Duan, X. Guo, Corros. Sci. 98 (2015) 500–506;
(b) L. Ren, S. Huang, C. Zhang, R. Wang, W.W. Tjiu, T. Liu, J. Nanopart. Res. 14 (2012) 940.

[53] T.E. Motaung, A.S. Luyt, F. Bondioli, M. Messori, M.L. Saladino, A. Spinella, G. Nasillo, E. Caponetti, Polym. Degrad. Stab. 97 (2012) 1325–1333.

[54] Y.-S. Ye, Y.-N. Chen, J.-S. Wang, J. Rick, Y.-J. Huang, F.-C. Chang, B.-J. Hwang, Chem. Mater. 24 (2012) 2987–2997.